

# Evidence for a Strong $\sigma/\pi$ Interaction in 3,4,7,8-Tetrasilacycloocta-1,5-diyne and 3,4,7,9,11,12-Hexasilacyclododeca-1,5,9-triyne

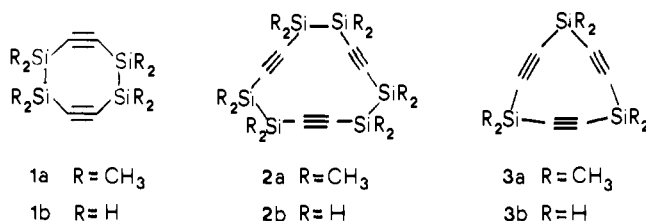
Rolf Gleiter,\*† Wolfgang Schäfer,† and Hideki Sakurai\*†

Contribution from the Institut für Organische Chemie, Universität Heidelberg,  
D 6900 Heidelberg, West Germany, and Department of Chemistry, Tohoku University,  
Sendai 980, Japan. Received September 12, 1984

**Abstract:** The photoelectron spectra of 3,3,4,4,7,7,8,8-octamethyl-3,4,7,8-tetrasilacycloocta-1,5-diyne (**1a**), 3,3,4,4,7,7,8,8,12,12-dodecamethyl-3,4,7,8,11,12-hexasiladodeca-1,5,9-triyne (**2a**), and 3,3,6,6,9,9-hexamethyl-3,6,9-trisilanonona-1,4,7-triyne (**3a**) have been recorded. The interpretation of the first bands of these spectra is based on the comparison with calculated orbital energies, according to the MINDO/3 and MNDO methods. A comparison between the orbital sequence of **1a** and that of cycloocta-1,5-diyne (**4**) shows a smaller through-space and a larger through-bond interaction for **1a**. The through-bond interaction between the in-plane  $\pi$  orbitals and the Si-Si  $\sigma$  bonds yields a strong destabilization of  $a_g(\pi)$ . A similar through-bond interaction is also observed in **2a**. A comparison between the PE spectra of **2a** and cyclododeca-1,5,9-triyne (**5**) shows a strong destabilization of the  $a_1(\pi)$  orbital in **2a**.

In systems with nonconjugated  $\pi$  bonds, we very often encounter a strong through-bond coupling of the  $\pi$  orbitals. Provided there is a rigid geometry, this interaction can be influenced by lowering or rising the effective basis orbital energies of the fragments. In the case of [2.2]paracyclophane, this has been demonstrated by replacing the two  $C_2H_4$  bridges either by two  $C_2F_4$  or by two  $C_3H_4$  (three-membered ring) units.<sup>2</sup>

In this paper, we make use of the effect that the Si-Si bond shows a very low ionization energy<sup>3</sup> and thus is ideally suited to destabilize  $\pi$  orbitals appropriately arranged, e.g., the  $\pi$  orbitals of the acetylenic moieties in 3,3,4,4,7,7,8,8-octamethyl-3,4,7,8-tetrasilacycloocta-1,5-diyne (**1a**)<sup>4</sup> and 3,3,4,4,7,7,8,8,11,11,12,12-dodecamethyl-3,4,7,8,11,12-hexasiladodeca-1,5,9-triyne (**2a**).<sup>5</sup>



The method of choice to probe the  $\sigma/\pi$  interaction in **1a** and **2a** is the He I photoelectron spectroscopy. To estimate the influence of an  $Si(CH_3)_2$  group upon the acetylenic moiety we also recorded the PE spectrum of 3,3,6,6,9,9-hexamethyl-3,6,9-trisilanonona-1,4,7-triyne (**3a**).<sup>5</sup> The PE spectra of **1a**, **2a**, and **3a** are shown in Figure 1. The PE spectrum of **1a** shows two peaks below 10 eV; the second one exhibits a shoulder at 9.05 eV (band ②) followed by a sharp peak at 9.4 eV (bands ③ and ④). The PE spectrum of **2a** shows one Gaussian-type peak at 8.4 eV well separated from a sharp and more intensive peak centered at around 9.4 eV followed by strongly overlapping bands at higher energy. The PE spectrum of **3a** shows one very intense sharp peak (bands ①-⑤) between 9.3 and 10 eV followed by a shoulder at 10.13 eV.

To assign the PE spectra we rely on Koopmans' approximation<sup>6</sup> which assumes that the recorded vertical ionization energies,  $I_{v,j}$ , can be set equal to the negative values of the orbital energies derived from a MO calculation on the ground state

$$I_{v,j} = -\epsilon_j$$

### PE Spectrum and Orbital Sequence of **3a**

Before we discuss the PE spectra of **1a** and **2a** and the corresponding MO pattern, we will discuss that of **3a**. In this compound

**Table I.** Comparison between the Measured Ionization Energies,  $I_{v,j}$ , of **3a** and the Orbital Energies,  $\epsilon_j$ , Calculated for **3b** Using the MINDO/3 and the MNDO Method (All Values in eV)

band	$I_{v,j}$	$-\epsilon_j(\text{MINDO}/3)$	$-\epsilon_j(\text{MNDO})$
①-⑤	9.3-10	9.22 ( $2a_2''$ ) 9.46 ( $4a_1'$ ) 9.91 ( $5e'$ )	10.49 ( $2a_2''$ ) 10.76 ( $4a_1'$ ) 10.78 ( $5e'$ )
⑥	10.13	9.96 ( $2e''$ )	10.83 ( $2e''$ )

**Table II.** Comparison between the Measured Ionization Energies,  $I_{v,j}$ , of **1a** and the Orbital Energies,  $\epsilon_j$ , Calculated for **1b** Using the MINDO/3 and the MNDO Method (All Values in eV)

band	$I_{v,j}$	$-\epsilon_j(\text{MINDO}/3)$	$-\epsilon_j(\text{MNDO})$
①	8.13	8.14 ( $5a_g$ )	9.51 ( $5a_g$ )
②	9.05	9.62 ( $2b_{2g}$ )	10.58 ( $2b_{2g}$ )
③	9.3	9.75 ( $2b_{1u}$ )	10.71 ( $2b_{1u}$ )
④	9.45	9.96 ( $4b_{3u}$ )	10.93 ( $4b_{3u}$ )
⑤	10.2	10.83 ( $3b_{2u}$ )	11.21 ( $3b_{2u}$ )

the interaction between the "in-plane" and "out-of-plane"  $\pi$  orbitals ( $\pi_i$  and  $\pi_o$ , respectively) and the  $\sigma$  frame is about the same as suggested by MINDO/3<sup>7</sup> and MNDO<sup>8</sup> calculations on **3b**. In Table I we list the predicted orbital energies, and in Figure 2 we show the corresponding wave functions. Both methods predict as the highest occupied MO's six wave functions belonging to the irreducible representations  $A_2''$ ,  $E''$ ,  $A_1'$ , and  $E'$  if we assume  $D_{3h}$  symmetry for **3b**. All six MO's are predicted to lie in a range of 0.4 to 0.6 eV (see Table I) in good agreement with experiment.

The "center of gravity" of bands ①-⑥ in the PE spectrum of **3a** yields a value of 9.7 eV. This value should be a good estimate of what energy we have to expect for those acetylenic  $\pi$ -MO's which are perturbed by the inductive and hyperconjugative effect of a  $Si(CH_3)_2$  group.

- (1) Heilbronner, E.; Maier, J. P. *Helv. Chim. Acta* **1974**, *57*, 151.
- (2) Gleiter, R.; Eckert-Maksić, M.; Schäfer, W.; Truesdale, E. A. *Chem. Ber.* **1982**, *115*, 2009.
- (3) Bock, H.; Ensslin, W.; Fehér, F.; Freund, R. *J. Am. Chem. Soc.* **1976**, *98*, 668.
- (4) Sakurai, H.; Nakadaira, Y.; Hosomi, A.; Eriyama, Y.; Kabuto, C. *J. Am. Chem. Soc.* **1983**, *105*, 3359.
- (5) Sakurai, H.; Eriyama, Y.; Hosomi, A.; Nakadaira, Y.; Kabuto, C. *Chem. Lett.* **1984**, 595.
- (6) Koopmans, T. *Physica* **1934**, *1*, 104.
- (7) Bingham, R. C.; Dewar, M. J. S.; Lo, D. H. *J. Am. Chem. Soc.* **1975**, *97*, 1255. Bischof, P. *Ibid.* **1976**, *98*, 6844.
- (8) Dewar, M. J. S.; Thiel, W. *J. Am. Chem. Soc.* **1977**, *99*, 4899.

\*Universität Heidelberg.

†Tohoku University.

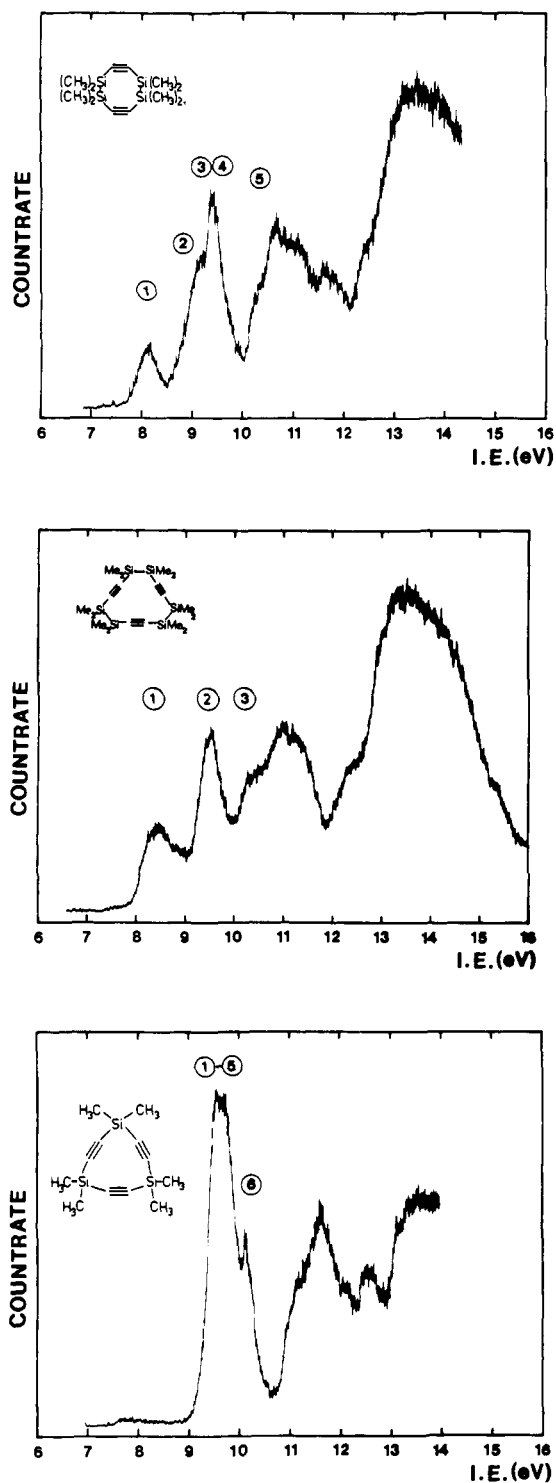


Figure 1. PE spectra of 1a, 2a, and 3a.

### PE Spectrum and Orbital Sequence of 1a

In Table II we have compared the ionization energies of the first five bands of 1a with the calculated orbital energies as derived from a MINDO/3<sup>7</sup> and a MNDO<sup>8</sup> calculation on the model 1b. We find a good agreement between experiment and the MINDO/3 results of 1b. In the case of the MNDO results, the sequence of the MO's agrees with that predicted by MINDO/3, the numerical agreement, however, being less good which is usually the case. According to the interpretation given, the first band is due to ionizations from the orbital which can be described as the bonding linear combination of the "in-plane"  $\pi$  orbitals destabilized by the Si-Si  $\sigma$  bonds ( $a_g(\pi_i^+)$ ). The HOMO is well separated from three close-lying MO's belonging to the irreducible representations  $B_{2g}$ ,  $B_{3u}$ , and  $B_{1u}$  if we assume  $D_{2h}$  symmetry for

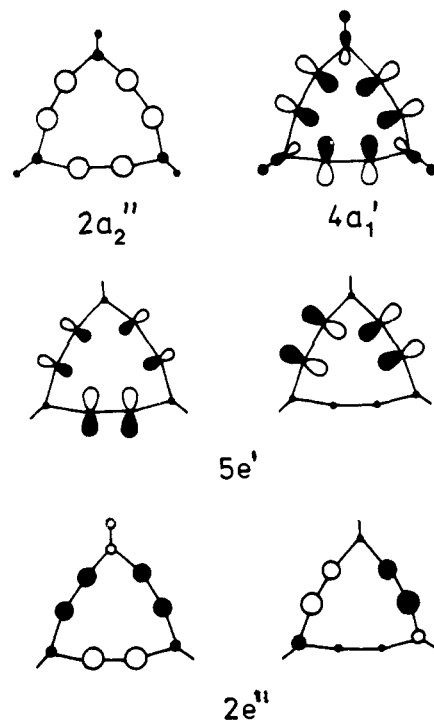


Figure 2. Schematic representation of the highest occupied canonical molecular orbitals of 3b.

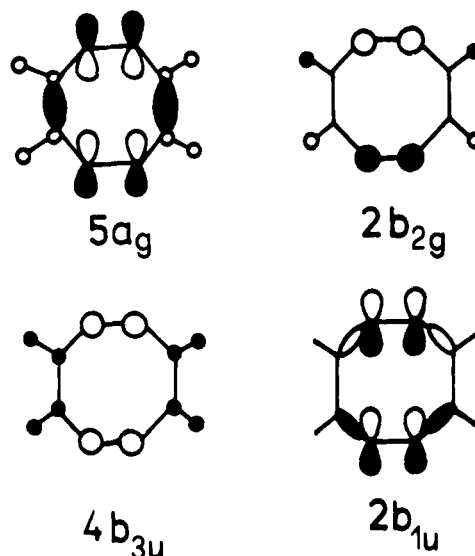


Figure 3. Schematic representation of the highest occupied canonical molecular orbitals of 1b.

1a.<sup>4</sup> The wave functions can be described as the bonding ( $\pi_0^+$ ) and antibonding ( $\pi_0^-$ ) linear combinations of the "out-of-plane"  $\pi$ -MO's and the antibonding ( $\pi_i^-$ ) linear combination of the "in-plane"  $\pi$  orbitals. All four wave functions are shown schematically in Figure 3.

To analyze the interaction between the two  $\pi$  systems (through-space) and between  $\pi$  and  $\sigma$  fragments (through bond), we proceed as in the case of cycloocta-1,5-diyne 4.<sup>9</sup>

The canonical MO's of 1b (see Figure 3) obtained by a MINDO/3 calculation are transformed into the localized MO's according to Edmiston and Ruedenberg.<sup>10</sup> The through-space interaction between the two "in-plane"  $\pi$  fragments  $\pi_i^1$  and  $\pi_i^2$  results from the off-diagonal element  $\langle \pi_i^1 | F | \pi_i^2 \rangle$  of the localized

(9) Bieri, G.; Heilbronner, E.; Kloster-Jensen, E.; Schmelzer, A.; Wirz, J. *Helv. Chim. Acta* **1974**, *57*, 1265.

(10) Edmiston, C.; Ruedenberg, K. *Rev. Mod. Phys.* **1963**, *35*, 457; *J. Chem. Phys.* **1965**, *43*, 597.

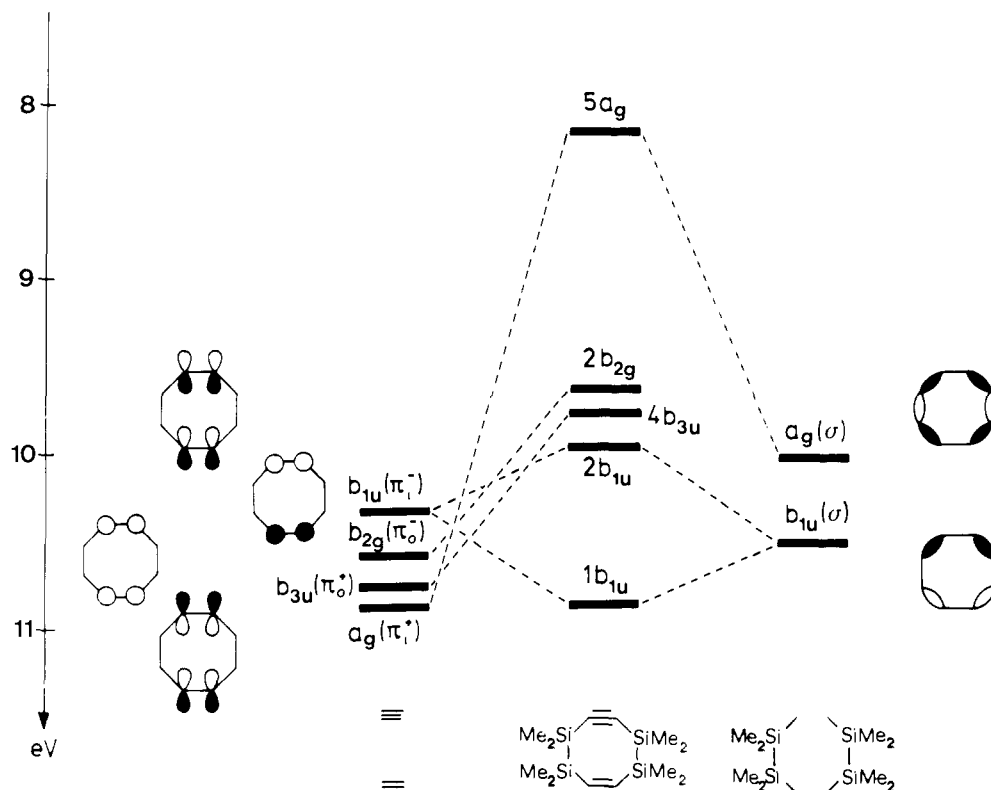


**Figure 4.** Interaction diagram between the symmetry-adapted localized  $\pi$  MO's (SLMO's) with precanonical  $\sigma$ -MO's (PCMO's) in **1b** to yield the canonical MO's. At the right the PE data of **1a** are shown.

Fock matrix  $F$ . A value of  $-0.28$  eV is calculated. In the case of **4** a value of  $-1.32$  eV has been derived according to a MINDO/2 calculation.<sup>9</sup> The smaller through-space interaction encountered for **1b** compared with **4** is due to the larger separation between the triple bonds in **1a** ( $3.25 \text{ \AA}$ ) compared with  $2.75 \text{ \AA}$  found for **1**.<sup>9</sup> The matrix elements for through-bond interaction between the in-plane  $\pi$  orbitals and the  $\sigma$  frame amounts to  $\langle \pi_i | \sigma \rangle = -1.19$  eV while the matrix element for the interaction between the out-of-plane  $\pi_0$  orbitals and the Si-H  $\sigma$  bonds amounts to  $\langle \pi_0 | \sigma' \rangle = -0.71$  eV.

The same calculation yields the following basis energies

$$\langle \pi_i | F | \pi_i \rangle = -10.61 \text{ eV}, \quad \langle \pi_0 | F | \pi_0 \rangle = -10.67 \text{ eV}$$

$$\langle \sigma' | F | \sigma' \rangle = -10.58 \text{ eV}, \quad \langle \sigma'' | F | \sigma'' \rangle = -11.80 \text{ eV}$$

In these matrix elements the expression  $\sigma'$  stands for the C-Si-Si-C fragment and  $\sigma''$  is localized at the Si-H bonds.

The factorization of the localized Fock matrix (into one block containing the four  $\pi$  orbitals and another one containing the  $\sigma$  orbitals) and subsequent diagonalization yields the symmetry-adapted semilocalized MO's (SLMO's). In the case of the  $\pi$  orbitals we obtain the four linear combinations shown on the left of Figure 4. The resulting two highest occupied precanonical (PCMO's)  $\sigma$  orbitals,  $a_g(\sigma)$  and  $b_{1u}(\sigma)$ , are shown on the right of Figure 4.

The interaction between the semilocalized  $\pi$  orbitals and  $\sigma$  orbitals of the same symmetry leads to the canonical MO's encountered in Figure 3. The corresponding interaction diagram is shown in the center of Figure 4. This diagram demonstrates a strong  $\pi/\sigma$  interaction between  $a_g(\pi_1^+)$  and  $a_g(\sigma)$ . This is mainly due to the small energy difference of the corresponding basis orbital energies  $a_g(\pi_1^+) = -10.89$  eV,  $a_g(\sigma) = -10.01$  eV. In the case of **4** the basis orbital energy for  $a_g(\sigma)$  is calculated to be  $-13.44$  eV and thus a smaller  $\pi/\sigma$  interaction results. The relatively moderate interaction between  $b_{1u}(\pi)$  and  $b_{1u}(\sigma)$  can be

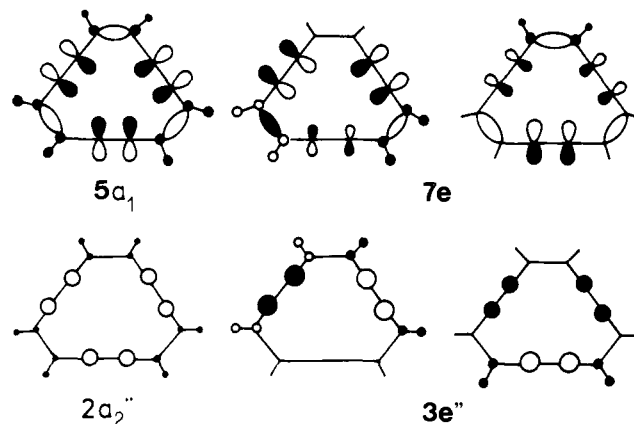


**Figure 5.** Schematic representation of the highest occupied canonical molecular orbitals of **2b**.

traced back to the reduced overlap between  $b_{1u}(\sigma)$  and  $b_{1u}(\pi^-)$  due to a C-C-Si angle of  $166^\circ$ .<sup>4</sup>

The destabilization of the out-of-plane  $\pi$ -MO's ( $\pi_0^+$ ,  $\pi_0^-$ ) encountered in Figure 4 can be explained by the hyperconjugative interaction with the neighboring Si-H bonds of the bridge in **1b**.

The assignment of bands ① to ⑤ to the  $\pi$ -MO's of **1a** is further corroborated by the position of the  $\pi$  bands in the PE spectrum of **3a**.

#### PE Spectrum and Orbital Sequence in **2a**

To understand the origin of the first bands in the PE spectrum of **2a**, we first consider the results of model calculations on **2b** using the MINDO/3<sup>7</sup> and MNDO<sup>8</sup> procedures. In Figure 5 we show the highest occupied canonical molecular orbitals of **2b** assuming  $D_{3h}$  symmetry. As anticipated from the discussion on **1b** we encounter a large mixing between the symmetry-adapted localized "in-plane"  $\pi$ -MO's and the Si-Si bonds of the  $\sigma$  frame while the out-of-plane  $\pi$ -MO's are only weakly disturbed by the Si-H bonds. Strongest is the mixing between  $a_1'(\pi_i)$  and a pre-

(11) Houk, K. N.; Strozier, R. W.; Santiago, C.; Grandour, R. W.; Vollhardt, K. P. C. *J. Am. Chem. Soc.* **1979**, *101*, 5183.

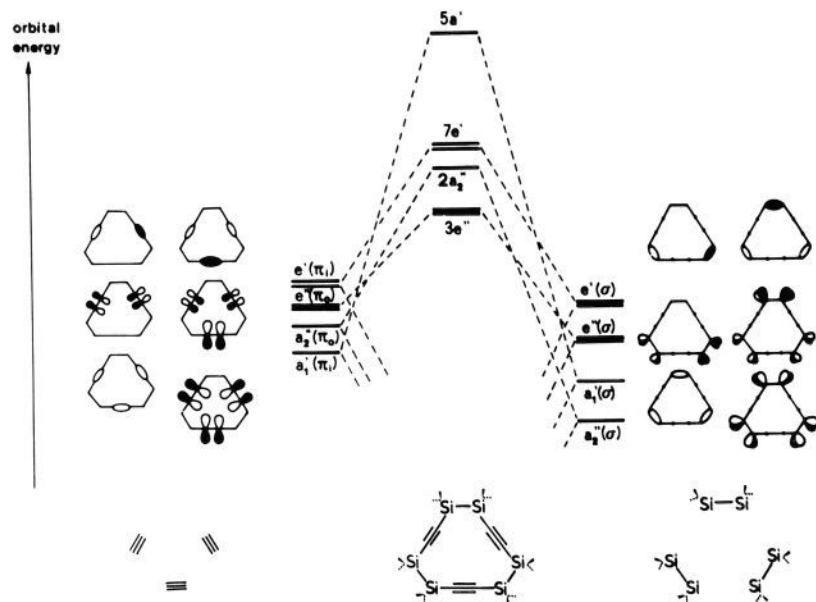


**Figure 6.** Qualitative interaction diagram between the symmetry-adapted localized molecular orbitals of three acetylenic units (left) with high-lying Si-Si- $\sigma$  MO's (right) to yield the highest occupied canonical MO's of **2a**.

**Table III.** Comparison between the Measured Ionization Energies,  $I_{v,j}$ , of **2a** and the Orbital Energies,  $\epsilon_j$ , Calculated for **2b** Using a ZDO Model and the MINDO/3 and the MNDO Method (All Values in eV)

band	$I_{v,j}$	$-\epsilon_j(\text{ZDO})$	$\epsilon_j(\text{MINDO}/3)$	$\epsilon_j(\text{MNDO})$
①	8.45	8.34 ( $5a_1'$ )	8.25 ( $5a_1'$ )	9.39 ( $5a_1'$ )
②	9.5	9.32 ( $7e'$ )	9.62 ( $7e'$ )	10.36 ( $7e'$ )
		9.72 ( $2a_2''$ )		
③	10.15	10.30 ( $3e''$ )	9.67 ( $3e''$ )	10.64 ( $3e''$ )

canonical  $\sigma$  orbital of the same irreducible representation. Adopting the same basis orbital energies for the  $\pi_1$ ,  $\pi_0$ ,  $\sigma'$ , and  $\sigma''$  fragments of **2b** as for **1b** and half of the value for the through-space interaction of the  $\pi_1$  and  $\pi_0$  fragments we obtain the following sequence of the canonical MO's:  $5a_1'$ ,  $7e'$ ,  $2a_2''$ , and  $3e''$  (see Table III).

In Figure 6 we show the corresponding qualitative interaction diagram between the symmetry-adapted linear combinations of the in-plane and out-of-plane ( $\pi_1, \pi_0$ )  $\pi$  orbitals of the three acetylenic moieties of **2** (left) with the high-lying precanonical  $\sigma$ -MO's centered at the Si-Si bonds (right). We encounter the strongest interaction between  $a_1'(\pi_1)$  and  $a'(\sigma)$  which leads to the HOMO.

Our ZDO-type calculation suggests the assignment of band ① in the PE spectrum of **2a** to one transition and band ② to three. With this assignment in line are the ratios below the peaks.

The two semiempirical methods predict a different sequence, namely  $5a_1'$  followed by  $7e'$ ,  $3e''$ , and  $2a_2''$  (see Table III). Due to the discrepancy between the ZDO model and semiempirical methods our assignment of bands ② and ③ given in Table III must remain tentative.

### Conclusions

Our results on **1** and **2** demonstrate nicely that the Si-Si  $\sigma$  bond is ideally suited to uncover strong  $\sigma/\pi$  interactions. In Figure 7 we have compared the PE results of **1a** with **4** and those of **2a** with cyclododeca-1,5,9-triyne (**5**).<sup>11</sup> While in the hydrocarbons **4** and **5** the  $\sigma$  and  $\pi$  levels are close together despite a strong  $\sigma/\pi$  interaction, this is not the case in **1** and **2**. The main difference for the enhancement in **1** and **2** is due to the fact that the basis orbital energies of the acetylenic moieties and the Si-Si  $\sigma$  bond are comparable and thus a strong interaction is possible.

Finally we would like to point out an interesting application of the strong destabilizing effect of the Si-Si  $\sigma$  bond, a [2.2]-paracyclophane bridged by two  $\text{Si}_2\text{Me}_4$  units (**6**). In this com-

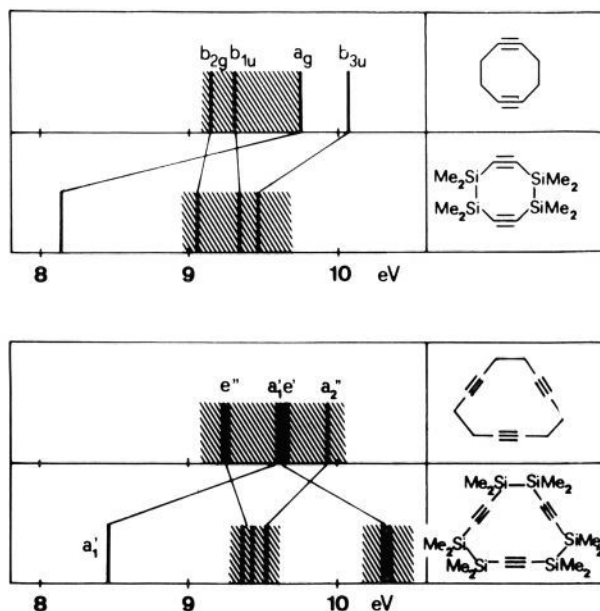
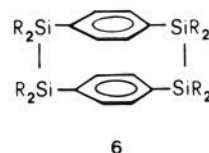


**Figure 7.** Correlation between the first bands of the PE spectra of **1a** and **2a** with **4** and **5**.<sup>11</sup>

pound the  $b_{3u}$  orbital is predicted to be well separated from the other two ( $b_{2g}$  and  $b_{3g}$ )  $\pi$ -MO's. This strong destabilization of  $b_{3u}$  should have interesting effects for the spectroscopic properties of **6**.



**6**

### Experimental Section

The preparation of the compounds **1a**–**3a** has been reported elsewhere.<sup>4,5</sup> The PE spectra of the pure samples were recorded at 60 °C (**1a**), 100 °C (**2a**), and 45 °C (**3a**) on a Perkin-Elmer PS 18 photoelectron spectrometer equipped with an He I light source. The spectra were calibrated with argon and xenon. An estimated accuracy of  $\pm 0.05$  eV

was achieved for the single bands and of  $\pm 0.1$  eV for the shoulders.

**Note Added in Proof.** The PE spectra of **1a** and **2a** have also been recorded by E. Kloster-Jensen and E. Heilbronner.

**Acknowledgment.** Financial support is gratefully acknowledged by the Deutsche Forschungsgemeinschaft, the Fonds der Chem-

ischen Industrie, and BASF Aktiengesellschaft in Ludwigshafen. We thank A. Flatow for measuring the PE spectra and G. G. for the drawings.

**Registry No.** **1a**, 85263-68-9; **1b**, 95465-41-1; **2a**, 89571-48-2; **2b**, 95483-61-7; **3a**, 91258-28-5; **3b**, 95465-42-2.

## Moments and the Energies of Solids

Jeremy K. Burdett\*<sup>1</sup> and Stephen Lee

Contribution from the Department of Chemistry, The University of Chicago, Chicago, Illinois 60637. Received May 21, 1984

**Abstract:** The use of the moments method applied to Hückel-based tight-binding theory is described. By locating  $n$ -rings in the middle of an  $m$  coordinate tree and calculating the energy difference of this structure compared to the simple tree itself, it is shown how the energy difference between two structures is controlled by the first few disparate moments of the density of states.  $\Delta E_r(X)$  curves are presented which describe the energetic difference between two structures whose first  $r-1$  moments are identical as a function of band filling ( $X$ ) ( $0 \leq X \leq 1$ ).

One of the fundamental problems associated with understanding the structure of solid-state systems is the connection between geometrical and electronic structure. Even in approximate theories, as simple as Hückel-based tight-binding theory, it is often difficult to correlate structural features with energetic effects. Much of this difficulty results, not from any inherent intransigence in the Hückel equations but from the complexity of the method of solution itself. As an example let us say we wish to determine the site preferences in an AB crystal associated with its two component atoms A and B, i.e., given a solid with two inequivalent sites,  $\alpha$  and  $\beta$ , which out of A and B will occupy these two sites as a function of the number of valence electrons. The standard method requires determination of the charge density at these crystallographically inequivalent sites.<sup>2</sup> To do this we must solve the Hückel equations at various points in  $k$  space and generate a set of eigenfunctions and eigenvalues. We need to use a fine enough mesh in  $k$  space (a large enough number of points) so that by reordering the eigenvalues by energy we create a reasonable approximation to the energy density of states. We then fractionate each eigenfunction as to its composition in terms of  $\alpha$ - and  $\beta$ -located orbitals, and integration via a population analysis leads to the charge density for a particular electron filling. Only then may we make predictions concerning the site preferences.

There are two arbitrary artifacts of this method of calculation, namely the use of  $k$  space and the generation of a large number of eigenfunctions, which have interposed themselves between the orbital topology of the system and the final structure prediction based on charge density. The development of new methods of solving the Hückel problem which obviates artificial concepts and relates structure and energy much more directly is certainly to be desired. Such a method has been in the physics literature for many years but more recently has been developed by several authors.<sup>3-7</sup> In this and the following two papers in this issue, we

shall use this technique to produce some very direct relationships between geometrical structure and electronic stability.

### Method of Moments

First, we define here our use of the term "Hückel" Hamiltonian (**H**). In this, and in the following two papers in this issue, we will consider systems whose energy bands, within the framework of tight-binding theory, may be obtained by solution of the secular determinant

$$|H_{ij}(k) - S_{ij}(k) \cdot E| = 0 \quad (1)$$

where  $H_{ij}(k)$  are the interaction and diagonal matrix elements of **H** linking the Bloch sums

$$\mu_i = N^{-1/2} \sum_j e^{ik \cdot R_{ij}} \chi_i(r - R_{ij}) \quad (2)$$

Here the  $\chi_i$  are the atomic basis orbitals contained within the unit cell. The sum is over all unit cells of the crystal  $j$ , where the orbital  $\chi_i$  is located on atoms residing at  $R_{ij}$  with respect to some arbitrary origin. The Coulomb integrals  $H_{ii} = \langle \chi_i | \mathcal{H} | \chi_i \rangle$  are usually estimated<sup>8</sup> from the relevant ionization potential and the interaction (or resonance) integrals by the Wolfsberg-Helmholz (or Mulliken) relationship

$$H_{ij} = \langle \chi_i | \mathcal{H} | \chi_j \rangle = \frac{1}{2} K S_{ij} (H_{ii} + H_{jj}) \quad (3)$$

where  $K$  is a constant and  $S_{ij} = \langle \chi_i | \chi_j \rangle$ , the overlap integral linking the atomic orbitals  $\chi_i$  and  $\chi_j$ . Our use of the descriptor "Hückel" refers to a calculation using eq 1 where the overlap integrals involving the Bloch sums are put equal to zero unless  $i = j$ ; i.e.,  $S_{ij}(k) = \delta_{ij}$ . The overlap integral is retained in the evaluation of the interaction elements in eq 3. The calculation is therefore an extended Hückel one but with neglect of overlap. In molecules, of course,  $S_{ij}(k) = S_{ij}$ .

The method of moments is based on the following two observations.<sup>3</sup>

(1)

$$\sum_i E_i^n = \text{Tr}(\mathbf{H})^n \quad (4)$$

where **H** is the Hückel Hamiltonian matrix,  $E_i$  is the  $i$ th eigenvalue

(8) E.g.; Burdett, J. K. "Molecular Shapes"; Wiley: New York, 1980.

(1) Camille and Henry Dreyfus Teacher-Scholar.  
 (2) See for example: Burdett, J. K. *Adv. Chem. Phys.* **1982**, *49*, 47.  
 (3) Cyrot-Lackmann, F. Thèse, Orsay, 1968.  
 (4) Ducastelle, F.; Cyrot-Lackmann, F. *J. Phys. Chem. Solids* **1970**, *31*, 1295; **1971**, *32*, 285.  
 (5) Cyrot-Lackmann, F. *J. Phys. Chem. Solids* **1968**, *29*, 1235.  
 (6) Cyrot-Lackman, F. *Surf. Sci.* **1969**, *15*, 535.  
 (7) Gaspard, J. P.; Cyrot-Lackmann, F. *J. Phys. C* **1973**, *6*, 3077.